IMPROVED GEM-MARS GCM WITH ATMOSPHERIC CHEMISTRY

F. Daerden, **L. Neary**, *Royal Belgian Institute for Space Aeronomy, Brussels, Belgium*, **R. T. Clancy**, *Space Science Institute, Boulder, Colorado, USA*, **M. D. Smith**, *NASA Goddard Space Flight Center, Greenbelt, Maryland, USA. (Frank.Daerden@aeronomie.be)*

Introduction

The Global Environmental Multiscale model for Mars (GEM-Mars) has undergone considerable improvements and now simulates Mars atmospheric chemistry in reasonable accordance with available datasets and with the LMD model [Lefèvre et al., 2004]. Model innovations include an update from GEM 3.3.0 to GEM 4.2.0, inclusion of radiative effects of water ice clouds, and a parameterization for non-condensable gas enrichment. The diurnal and seasonal variations are compared to observations and to other models.

1. The GEM-Mars GCM

The GEM-Mars General Circulation Model (GCM) is based on the Canadian Global Environmental Multiscale (GEM) model for weather forecasting on Earth [Côté et al., 1998; Daerden et al., 2015]. The model is typically operated on a grid with a horizontal resolution of 4°×4° and with 103 hybrid vertical levels reaching from the surface to ~150 km. Processes that were added to the model since older versions include lifting of size-distributed dust by saltation and in dust devils, and dust radiative heating using the refractive index of Wolff et al. [2006, 2009], an interactive CO_2 cycle with surface exchange, a multi-layered thermal soil model, turbulent transport in the atmospheric surface layer, convective transport inside the PBL, convection in the free troposphere through mixing of dust-generated instabilities, low level blocking, gravity wave drag, and a full water cycle with ice and surface frost formation, sedimentation of monodisperse particles, a subsurface ice table and radiative effects of clouds and surface ice. The geophysical boundary conditions include topography [Smith et al., 1999], albedo [Christensen et al., 2001], thermal inertia [Putzig et al., 2005], and roughness length [Hébrard et al., 2012]. The integration timestep was 1/48 of a sol (Martian solar day).

2. The dust cycle

The implementation of saltation in the model uses the “KMH” method of Kahre et al. [2006] with the application of a detailed roughness map [Hébrard et al., 2012; Daerden et al., 2015]. The mass flux from dust devils is implemented by the parameterization of Renno et al. [1998]. Both methods require tuning of proportionality factors to match observations. The resulting simulated seasonal dust cycle (Fig. 1) compares qualitatively to observations, e.g. from THEMIS on Mars Odyssey [Smith, 2009] (note that dust inside the polar nights remains largely unobserved). Settings were applied for a year with minor dust storm activity.

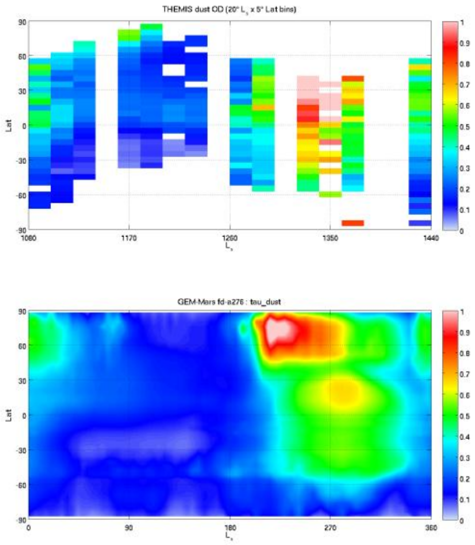

Figure 1: Zonal mean optical depth of dust simulated in GEM-Mars for a year with minor dust storm activity, compared to dust optical depth observations from THEMIS on Mars Odyssey for Mars year 31.

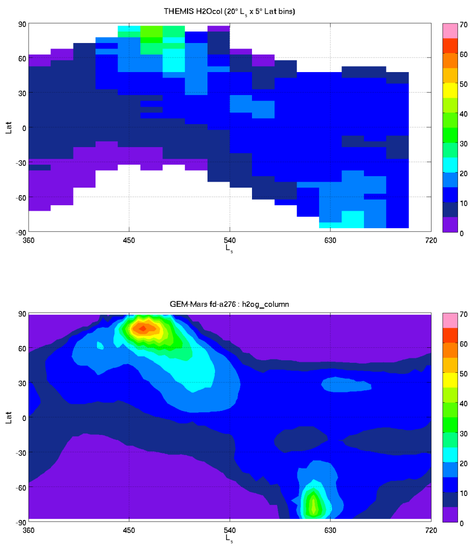

Figure 2: Seasonal cycle of the zonally averaged total water column (in pr-μm) as observed by CRISM in Mars year 30 (top) and simulated by GEM-Mars (bottom).

3. The water cycle

Together with the global circulation patterns, the Mars water cycle is the principle driver of the Martian photochemistry. The simulated water cycle is compared in Fig. 2 to the observations by the Compact Reconnaissance Imaging Spectrometer for Mars (CRISM) instrument [Smith et al., 2009] on the NASA Mars Reconnaissance Orbiter (MRO).

4. The ozone cycle

The seasonal cycle of ozone is strongly controlled by the water cycle. The simulated cycle is shown in Fig. 2 and compared to the observations by the Mars Color Imager (MARCI) instrument [Clancy et al., 2016] on MRO. The results shown here do not include heterogeneous chemistry processes, as was suggested in Lefèvre et al. [2008].

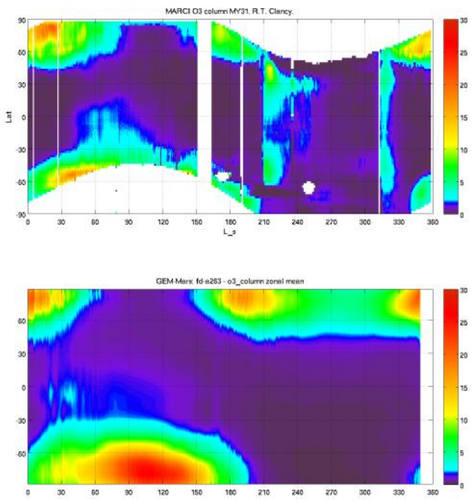

Figure 3: Seasonal cycle of the zonally averaged total ozone column (in µm-atm) as observed by MARCI in Mars year 31 (top) and simulated by GEM-Mars (bottom). Elevated values at nonpolar latitudes in the second half of the year in the MARCI data are due to dust contamination in the retrieval process [Clancy et al., 2016].

5. Seasonal cycle of noncondensable species

Because CO_2 as major atmospheric constituent is subject to dramatic condensation during the polar winters, the resulting effect on the mixing ratios of species that do not condense with CO_2 is considerable [Sprague et al., 2004; Smith et al., 2009]. In GEM-Mars a parameterization was developed to simulate this process based on the local pressure change upon CO_2 condensation or evaporation. The resulting seasonal cycle of carbon monoxide (CO) is shown in Fig. 4 and compared to CRISM data from Mars year 30 [Smith et al., 2009].

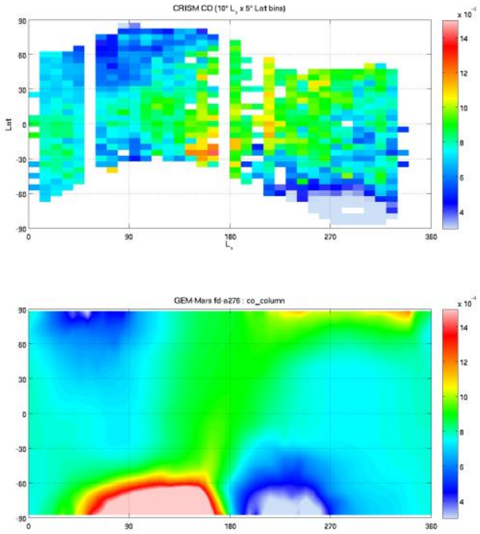

Figure 4: Zonal mean column-averaged volume mixing ratio of carbon monoxide observed by CRISM in Mars year 30 (top) compared to the simulation in GEM-Mars (bottom).

References

Christensen, P. R., et al. (2001), J. Geophys. Res. 106, 23,823-23,871.

Clancy, R. T., et al. (2016), Icarus 266, 112–133

Côté, J. et al. (1998), Mon. Weather Rev., 126, 1373–1395.

Daerden, F. et al. (2015), Geophys. Res. Lett., 42, doi:10.1002/2015GL064892.

Hébrard, E. et al. (2012), J. Geophys. Res., 117, E04008, doi:10.1029/2011JE003942.

Kahre, M. A. et al. (2006), J. Geophys. Res., 111, E06008, doi:10.1029/2005JE002588.

Lefèvre, F. et al. (2004), J. Geophys. Res., 109, E07004, doi:10.1029/2004JE002268.

Lefèvre, F., et al. (2008), Nature 454, 971–975

Putzig, N. E., et al. (2005), Icarus 173, 325-341, 10.1016/j.icarus.2004.08.017.

Renno, N. O. et al. (1998), J. Atmos. Sci., 55, 3244.

Smith, D. E., et al. (1999), Science 284, 1495, doi: 10.1126/science.284.5419.1495.

Smith, M. D. (2004), Icarus, 167, 148–165.

Smith, M. D. (2009), Icarus 202, 444–452

Smith, M. D., et al. (2009), J. Geophys. Res., 114, E00D03, doi:10.1029/2008JE003288.

Sprague, A. L., et al. (2004), Science 306, 1364, DOI: 10.1126/science.1098496

Wolff, M. J., et al. (2006), J. Geophys. Res., 111, E12S17, doi:10.1029/2006JE002786.

Wolff, M. J., et al. (2009), J. Geophys. Res., 114, E00D04, doi:10.1029/2009JE003350.